Tanganelli et al., *Cogent Engineering* (2017), 4: 1371578
https://doi.org/10.1080/23311916.2017.1371578

cogent engineering

CIVIL & ENVIRONMENTAL ENGINEERING | RESEARCH ARTICLE

On the modelling of infilled RC frames through strut models

Marco Tanganelli[1], Tommaso Rotunno[1] and Stefania Viti[1]*

Received: 20 July 2017
Accepted: 22 August 2017
First Published: 06 December 2017

*Corresponding author: Stefania Viti, Department of Architecture (DiDA), University of Florence, Via della Mattonaia 14, 50121 Firenze, Italia
E-mails: viti@unifi.it, vitistef@gmail.com

Reviewing editor:
Paolo Zampieri, Universita degli Studi di Padova, Italy

Additional information is available at the end of the article

Abstract: Infill panels largely affect the seismic response of framed constructions. The wide variety in their mechanical and geometrical features has produced many different models and assumptions in their analytical representation. In this paper the simplest and most diffuse analytical approach, based on the introduction of equivalent struts, has been checked. An overview is presented, focusing on the strut dimensions, strength and number. Two case-studies, taken by two different experimental campaigns, have been considered and reproduced. The obtained results have been compared to the experimental ones, and some parameters have been checked for selecting the model to use for analysis.

Subjects: Structural Mechanical Engineering; Structural Engineering; Architecture; Building and Construction

Keywords: infilled RC frames; strut-model, masonry infill panels; nonlinear response of infilled constructions; strut strength

1. Introduction

Infilled frame constructions have been extensively built during the last 200 years. The large diffusion of this type of buildings induced both an high interest of the scientific community in the evaluation

ABOUT THE AUTHORS

The authors deal with the seismic assessment of existing buildings, both historical and modern ones, constructed before the current seismic legislation was passed. In Italy most part of buildings have been constructed without attending anti-seismic prescriptions; therefore, a reliable evaluation of their seismic performance is an essential step for a convenient choice about their use and maintenance. The research group deals with the main issues related to the numerical modeling of pre-normative buildings, such us: (1) mechanical properties of materials, (2) inelastic involvement of the structure, (3) effects of the uncertainties affecting the constructive process, (4) effects related to nonstructural components and (5) role of the soil on the effective seismic input. This paper is focused on the role of the masonry infill panels on the seismic performance of RC framed constructions. Infill panels, indeed, largely affect the seismic assessment of constructions, despite they have been usually neglected in the modeling; furthermore, their contribution is still quantified without a strict procedural prescription.

PUBLIC INTEREST STATEMENT

Infill panels largely affect the seismic response of framed constructions. The wide variety in their mechanical and geometrical features has induced, in the last decades, many different models and assumptions in their analytical representation. In this paper the simplest and most diffuse analytical approach, based on the introduction of equivalent struts, has been checked. Some of the main strut models have been presented and compared as regards the number, the dimensions and the strength to assume for the equivalent strut. The numerical results provided by the considered models by performing a nonlinear static analysis have been checked with reference to two different case-studies, differing to each other for the ratio between the infill and the frame stiffness and strength. The comparison between experimental and numerical data, expressed in terms of stiffness and strength, has pointed out the role of each considered assumption in the effectiveness of the models.

of their seismic performance and a wide variety in their properties. The mechanical behavior of an infilled framed structure, indeed, depends on the mechanical properties of the structure and of the infill panels, but even on their mutual stiffness and the type of adopted connections, which can induce different collapse scenarios. Moreover, it is well known that masonry presents itself a wide variety of possible performances, due to the multiple combination among the constituting materials, and therefore having a behavior difficult to be predicted. As a consequence, many different analytical procedures have been developed to represent the seismic behavior of the infilled frames, based on the observation of the mechanical properties of the single microelements constituting the system, or on a macroscopic approximated representation.

Moreover, the "quality" of the infill panels contribution to the seismic response of framed structures is not obvious; the infill panels, in fact, increase the lateral stiffness and strength of the buildings, with a consequent improvement of their safety. But some of the effects can be detrimental for the seismic response of the building, since the collapse—or detachment—of the infill panels can induce a reduction in ductility, with a possible activation of local collapse mechanisms. In the representation of the mechanical contribution of the infill panels to the seismic response of framed constructions, therefore, the evaluation of the safest assumptions is not easy to pursue.

All the main International Technical Codes state the importance of including the infill panels in the representation of the seismic response of framed buildings. Nevertheless they differ with each other about the provided instructions for the representation. Eurocode 8 (EC 8-3, 2005) prescribes to take into account the infill panels contribution, without specifying the model to adopt to this purpose. The Federal Emergency Management Agency Code (FEMA 306, 1998; FEMA 356, 2000) suggests to represent the infill panels contribution by introducing equivalent pin-jointed diagonal struts, having the same thickness and mechanical properties than the infill panels. Besides, the frame members are required to resist to the further internal forces induces by the equivalent strut.

The "equivalent strut" approach is the simplest way to account for the infill panels contribution; it has been introduced about 60 years ago (Holmes, 1961; Stafford Smith, 1966), and it is extensively used right now. The assumed cross section of the equivalent strut is usually fixed on the basis of the geometrical and mechanical properties of the infill material (Holmes, 1961; Mainstone, 1971), whilst the post-cracking behavior of the strut can be determined on the basis of experimental tests (Cavaleri & Di Trapani, 2015; Reinhorn, Madan, Valles, Reichman, & Mander, 1995), or by comparing the macro-model results to the ones provided by nonlinear FE analysis (Asteris, Kakaletsis, Chrysostomou, & Smyrou, 2011; Durrani & Luo, 1994; Fardis, 1996). Since the point-jointed single strut does not provide any information about the distribution of shear force in the columns, equivalent multiple-struts models (Ali, 2009; Crisafulli, 1997; El-Dakhakhni, Elgaaly, & Hamid, 2003; Uva, Raffaele, Porco, & Fiore, 2012) have been also developed.

Many different—single and multiple—strut models have been proposed in these years, providing a large range of width for the diagonal strut. Moreover, the strength of the strut can be defined according to different assumptions, which refer to alternative collapse mechanisms of the panel. An exhaustive state of art of all possible analytical approaches to the problem of the infilled panels representation would be an arduous work, and is beyond the aim of this paper. This work is aimed at evaluating a range of variability, and the consequent possible reliability, of the standard strut models in representing simple infilled frames. Various formulations of strut models and alternative strength values of the infill have been compared, in order to evaluate, in term of maximum capacity, the range of results related to the more common assumptions. The considered assumptions have been applied to two different case-studies, which have been chosen after two different experimental surveys, respectively made by Al-Chaar, Issa, and Sweeney (2002) and Zhai, Kong, Wang, and Chen (2016). The two considered frames present different mechanical properties; namely, their ratio between the infill panel and the frame stiffness is very different to each other.

The results found for the considered case-studies have been presented in Chapter 4. The capacity curves found by adopting all the considered assumptions in terms of strut width, stress and number have been shown and compared to the corresponding experimental curves. The comparison has been checked in terms of elastic stiffness and maximum base shear, which can be assumed as the most representative response quantities. In Chapter 5 the role of each of the considered assumptions, i.e. the strut width, strength and number, has been checked, in terms of amount of scatter in results related to each choice. Finally, a joined lecture of the two case-studies has been proposed to evaluate a suitable criterion to select the strut-model to use for analysis.

2. The considered strut models assumptions

The structural behavior of infilled frames under horizontal actions represented through strut-models depends on three main issues (Chrysostomou & Asteris, 2012; Uva et al., 2012), i.e. the width and the mechanical characterization of the strut, which determine the stiffness and strength assumed for the panel, and the model setting, i.e. the number of the introduced struts and the consequent description of each of them. In the following sections each of these issues has been presented. In Figure 1 a standard scheme of an infilled frame is shown, and the main symbols used in the following paragraphs to indicate the main geometrical and mechanical quantities are reported.

2.1. Strut width, w

Several contributions have been dedicated to the evaluation of the strut width. An exhaustive gathering of all the expressions set in these decades to quantify the width of the equivalent strut in beyond the scope of this work. Usually the thickness of the strut, t_{inf}, is assumed to coincide to the panel one, whilst the width of the panel is defined after the panel dimension. Holmes (1961), as well as Paulay and Priestely (1992), proposed to relate the strut width directly to the diagonal length (see Table 1). Most part of strut models, however, assume more complex relationships to quantify the strut width. An important parameter for infill panels classification is the dimensionless quantity λ_h,

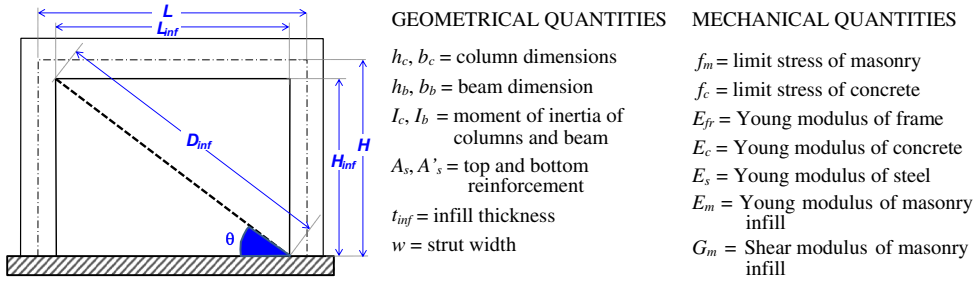

Figure 1. Scheme of a standard frame and notation of the main quantities.

Table 1. Width quantification according to the considered models

Model	Code	Width expression	Further specifications
Holmes (1961)	H	$D_{inf}/3$	
Mainstone (1971)	M	$0.175(\lambda_h H)^{-0.4} D_{inf}$	
Decanini and Fantin (1986)	D&F_UN	$(0.748/\lambda_h + 0.085)D_{inf}$	$\lambda_h < 7.85$
		$(0.393/\lambda_h + 0.130)D_{inf}$	$\lambda_h > 7.85$
	D&F_CR	$(0.707/\lambda_h + 0.010)D_{inf}$	$\lambda_h < 7.85$
		$(0.470/\lambda_h + 0.040)D_{inf}$	$\lambda_h > 7.85$
Paulay and Priestly (1992)	P&P	$D_{inf}/4$	
Liaw and Kwan (1984)	L&K	$\frac{0.95Hcos}{(\lambda_h H_{inf})^{0.5}}$	
Durrani and Luo (1994)	D&L	$\gamma\sqrt{(L^2+H^2)}\sin(2\theta)$	where: $= 0.32\sqrt{\sin 2\theta}\left(\frac{H_{inf}^4 E_m t}{m E_c I_c H}\right)$ $m = 6\left(1+\frac{E_c I_b H}{E_c I_c L}\right)$
Chrysostomou and Asteris (2012)	C&A	$0.270(\lambda_h)^{-0.4} D_{inf}$	

introduced by Stafford Smith (1966), which expresses the ratio between the panel and the frame stiffness, where the symbols in formula are described in Figure 1:

$$\lambda_h = H\left[\frac{E_m\, t_{inf} \sin(2\theta)}{4\, E_{fr}\, I_c\, H_{inf}}\right]^{\frac{1}{4}} \quad (1)$$

Based on the experimental and analytical data, Mainstone (1971) proposed a relationship between λ_h and the strut width, which has been adopted by the FEMA guidelines (FEMA 306, 1998).

Some other researchers proposed to relate the strut width to the stress attained by the panel. Decanini and Fantin (1986) observed a correlation between the stress level in the panel and its capacity to carry lateral loads (Flanagan & Bennett, 1999; Stafford Smith & Carter, 1969), and they provided two alternative expressions depending on the achievement of the panel cracking point. Durrani and Luo (1994) also proposed a semiempirical equation, on the basis of the experimental work of Mainstone (1974) and detailed numerical FEM analyses, by account for the stiffness of both beam and column of the frame.

2.2. Strut mechanical properties: E_m, f_m

According to the strut models, the stiffness of the infill panels depends on the strut dimensions and on the modulus of elasticity assumed for the infill material. Different relationships, very different from each other (see Table 2), are available to quantify the modulus of elasticity (E_m) of masonry. The stiffness of masonry panels, indeed, can vary very much depending on the mutual properties of bricks and mortar. Due to large scatter in the E_m evaluation, several researchers converge to the simple equation: $E_m = 1{,}000\, f_m$, i.e. the same relationship adopted for concrete infills. In this work, the values of the elastic modulus of the equivalent strut have been defined according to this last relationship.

The quantification of the strut strength to assume for the infill representation is even more complex and controversial, and a large variety of values can be found in the technical literature. This wide scatter of strength values depends on the difficult prediction of the physical behavior of the system "frame + infill panel", which depends, in turn, on the specific and mutual properties of bricks, mortar and frame geometry, mechanical properties, strength and ductility. Since different collapse mechanisms can occur, a single and univocal value able to represent the strut performance is hard to find. This problem is usually faced by considering alternative strength values to assume for representing the infill behavior, depending on the assumed collapse mechanism.

The infill collapse is usually related to three different in-plane mechanisms, despite even the out-of-plane failure can be possible (FEMA 306, 1998), under certain conditions. Such mechanisms are bed-joint sliding, diagonal tension and corner crushing.

The first cracking is usually related to the shear force in the panel, and it results in a stair stepped pattern of cracks in the mortar along the infill diagonal. For strong mortar, comparing to the units, the cracks show a linear trend, crossing both mortar and units, along the diagonal (diagonal cracking). For mortar much weaker of the units, instead, the cracks can propagate along the horizontal beds instead presenting a diagonal pattern (bed-joint sliding), leading to a more diffuse strength transfer between the panel and the surrounding frame. When the panel is sufficiently strong in shear, it can contribute to the global capacity of the system even after the cracking, until the crushing of the compressive corners along the panel diagonal (corner compression).

Table 2. E_m quantification

FEMA 306 suggestion (1998)	$E_m = 550\, f_m$
Paulay and Priestly (1992)	$E_m = 750\, f_m$
Hendry (1990)	$E_m = 2{,}116\, f_m^{0.50}$
Sinha and Pedreschi (1983)	$E_m = 1{,}180\, f_m^{0.83}$
Paulay and Priestly (1992), Sahlin (1971) and Smyrou (2006)	$E_m = 1{,}000\, f_m$

FEMA 306 is one of the International Code more supportive in the analysis of infilled frames by means of strut models. It indicates four limit conditions for the infill panel in the plane, referred to as much collapse scenarios, respectively related to sliding shear, compression, diagonal tension and general shear. The limit conditions are expressed in terms of the ultimate shear of the panel, and they refer to different resistant mechanisms.

The *diagonal cracking* (*DC*) failure is expressed by the following expression of the limit shear V_{DC} (FEMA 396, Equations 8–11) (FEMA 306, 1998):

$$V_{DC} = \frac{2\sqrt{2}\,L_{inf}t_{inf}f_m/40}{\frac{L_{inf}}{h_{inf}} + \frac{h_{inf}}{L_{inf}}} \tag{2}$$

based on to the Mohr-Coulomb failure theory, after the assumption of a cracking stress equal to 1/20 of the expected strength of masonry in the horizontal direction, f'_{m90}, assumed in turn equal to 50% f_m. Since in this work the numerical analyses are performed on strut-models only, a stress value for the strut has been found, by expressing the maximum force in the diagonal strut (D_{DC}) as $D_{DC} = V_{DC}$ / cos θ and by assuming an uniform stress distribution in the strut, i.e. $f_{DC} = D_{DC}/(t_{inf}\,w)$.

The *bed joint sliding* (*BJS*) usually occurs in conjunction with other failure modes and it is quantified according to the Mohr-Coulomb failure criteria. The expression provided by FEMA 306, modified according to (Alva, Kaminski, Mohamad, & Silva, 2015), provides the following limit condition:

$$V_{BJS} = \frac{\frac{f_m}{40} + 0.5\sigma_g\mu}{1 - \mu\, tg\theta} \tag{3}$$

Where σ_g is the vertical stress due to the self-weight of the panel and μ is the coefficient of friction. Even in this case, the axial capacity of the strut, D_{BJS}, can be determined as $D_{BJS} = V_{BJS}/\cos\theta$, and the strut stress f_{BJS} is expressed as $f_{BJS} = D_{BJS}/(t_{inf}\,w)$.

The *corner compression* (*CC*) failure is defined on the basis of a strut-model, where the width is quantified according to the Mainstone (1971) proposal, and the compressive stress in the strut, f_{CC}, is assumed to be equal to the expected strength of masonry in the *horizontal* direction, $f'_{m90} = 0.5\,f_m$.

Several further formulations could be assumed for the width capacity quantification, provided by as much researchers. Special attention should be paid to the contribution given by Crisafulli (1997), who proposed suitable stress formulation based on the Mann and Muller (1982) theory, appositely modified. The Mann and Muller theory studies the behavior of unreinforced masonry after shear and compressive stresses, based on equilibrium considerations. It assumes that stress parallel to the bed joints can be neglected, so that no shear stress can be transferred by the head joints and a uniform distribution of shear and compressive stress inside the masonry panel. Crisafulli modified this last assumption, suggesting an alternative linear distribution, shown in Figure 2.

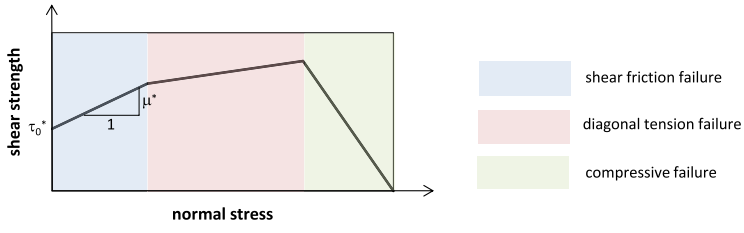

Figure 2. Stress distribution in the masonry infill panel suggested by Crisafulli (1997).

The limit stress values provided by Crisafulli (1997) refer to three different collapse mechanisms, related to the attainment of as much as limit stress values inside the strut, i.e. the shear friction (f_{SF}), the diagonal tension (f_{DT}) and the compressive (f_c) ones. According to this approach, the stress to assume for the strut is the minimum among the three limit values. For standard geometries, i.e. for θ below 87° (Crisafulli, 1997) the collapse mechanisms are related to shear friction or diagonal tension only, and therefore the possible stress values to assign to the strut are provided by the following relationships:

$$f_{SF,\theta} = \frac{\tau_0^*}{\sin\theta\left(\cos\theta - \mu^* \sin\theta\right)} \tag{4}$$

$$f_{DT,\theta} = \frac{f_t}{\sin\theta\left(C_s \cos\theta - 0.27 \sin\theta\right)} \tag{5}$$

where τ* and μ* are defined as (Crisafulli, 1997) Equation 4.17):

$$\tau_0^* = \frac{\tau_0}{1 + \mu\, C_n b/d} \tag{6}$$

$$\mu^* = \frac{\mu}{1 + \mu\, C_n b/d} \tag{7}$$

and C_n and C_s are coefficients determined by means of experimental analyses, and assumed equal to 1.5 and 2.0 respectively, while d and b are the brick length and height.

Liuaw and Kwan (1983a, 1983b) have derived different formulations for the limit stress values to assume for analysis of strut models, based on the plastic collapse theory. Even their approach considers three different collapse mechanisms, i.e. the corner crushing with failure in the column, the corner crushing with failure in the beam and the diagonal crushing mode.

2.3. Strut number

The number of struts to adopt in the modeling of infilled frames depends on the purpose of the analysis, and on the quality of the expected information. The most common models are made by 1 strut only; they are made by 1 strut for each frame diagonal (i.e. two struts for each frame), since they are assumed to be active only after compressive forces. The adoption of struts effective after compression only is usually acceptable, since the bond strength at the panel-frame interfaces and the tensile strength of the masonry are very low. In this case, therefore, only low tensile actions can be transferred.

The point-jointed 1-strut models can provide affordable information about the increase and distribution in shear force in the columns due to the infill panel interaction. To overcome this limitation, multiple-struts models (Ali, 2009; El-Dakhakhni et al., 2003; Uva et al., 2012) can be adopted, or additional restraints can be introduced at the ends of the strut (Mosalam & Ayala, 1996).

The need to know the effective stress distribution in the areas next to the corner among column, beam and diagonal strut induces to represent the system through multiple struts. The multiple-struts models (see Figure 3) consist in introducing two or three (for each direction) diagonal struts. In this way the amount of axial load in the struts is found together with the effective shear distribution in the members, with a consequent consistency between these quantities.

In multiple-struts models, the mutual distance between two consecutive struts, z, introduced by Stafford Smith (1966), plays an important role, since it influences the stress distribution in the frame, indicating the areas subjected to shear concentration, where an higher ductility is required.

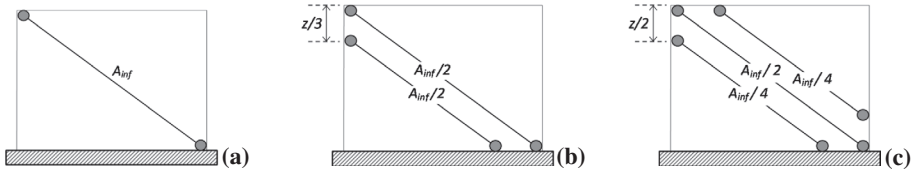

Figure 3. Strut models: a. 1-strut b. 2-strut c. 3-strut.

where $z = \pi H/2\lambda_H$ is the contact lenght, λ_H is found according to eq. (1) and A_{inf} is the masonry strut area (t_{inf} w)

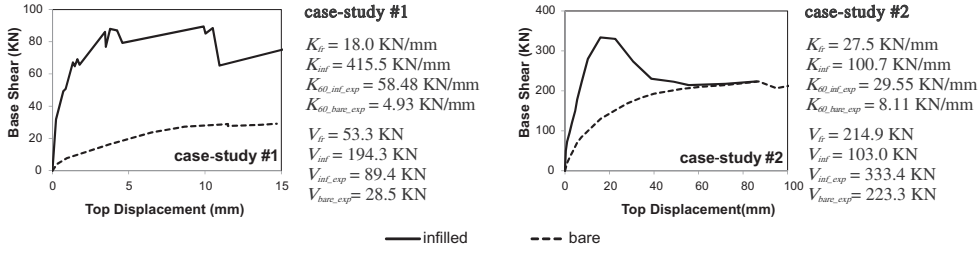

Figure 4. Experimental behavior of the two case-studies.

Usually the total area of all the struts, A_{inf}, is assumed to be the same of the single strut one, i.e. equal to the product of the thickness *t* and the width, w, quantified according to § 2.1, and each of the lateral struts are assume to have the 25% of the total stiffness, whereas the remaining 50% quote is assigned to the central one (Crisafulli, 1997; Verderame, De Luca, Ricci, & Manfredi, 2011). More complex models, having an higher number of struts or different geometry or resistant mechanisms (Crisafulli & Carr, 2007; El-Dakhakhni et al., 2003; Rodrigues, Varum, & Costa, 2010) can also be adopted.

3. The case-studies

Two different case studies have been considered in this work, belonging respectively to the experimental campaigns performed by Al-Chaar et al. (2002) and Zhai et al. (2016). The two considered systems differ to each other very much, as regards geometry, mechanical properties and relative stiffness between infill and frame.

The frame #1 (Al-Chaar et al., 2002) is made of reinforced concrete, and it has an infill panel made of bricks masonry, presenting high stiffness and strength. The experimental results have been found by means an in-plane monotonic loading, without any additional vertical loads, and the system can be assumed as scaled 1:2 comparing to the current dimensions of infilled frames. The case-study #2 (Zhai et al., 2016) is made of a reinforced concrete frame and a concrete blocks infill. The frame can be considered to be in scale 1:1, and it has been subjected to cyclic loading, besides a vertical load. The detailed description of the two case-studies can be found in the indicated references. In the following sections the presentations of the two case-studies is limited to the information required for performing the analysis presented in Chapter 4.

3.1. Geometrical and mechanical description of the case studies

The experimental responses of the two case-studies, both the bare and the infilled ones, such as the shear force (V_{bare_exp}, V_{inf_exp}) and the elastic stiffness, measured for shear equal to 60% of the maximum ($K_{60\_bare\_exp}$, $K_{60\_inf\_exp}$), are shown in Figure 4. The two systems evidence a behavior very different each other: in the case-study #1 the capacity of the infilled system is more than three times the bare frame one. Furthermore, the capacity of the system remains much larger of the bare frame's one even after the infill cracking. The system does not achieve large displacements, due to the predominant role of the masonry panel, characterized by a brittle behavior. The behavior of the case-study #2 is more typical of a RC frame, with a larger base shear and top displacement, and a smaller contribution of the infill panel, which vanishes after the panel collapse. The two systems differ especially for the different role of the infill panel: in the first case the masonry infill plays the main role in the global behavior, whilst in the second one the infill panel, made of lighten concrete blocks, does not vanish the frame ductility. In Tables 3 and 4 all the main geometrical and

Table 3. Geometrical data of the case-studies

	L	H	L_{inf}	H_{inf}	t_{inf}	θ	H/L
	mm	mm	mm	mm	mm	rad	dimensionless
Case-study #1	2,032	1,425	1,829	1,327	57	0.628	0.75
Case-study #2	3,150	3,000	2,800	2,600	190	0.748	0.95

Table 4. Mechanical data of the case-studies

	f_c	τ_c	E_c	f_s	E_s	f_m	E_m
	N/mm^2	N/mm^2	N/mm^2	N/mm^2	N/mm^2	N/mm^2	N/mm^2
Case-study #1	38,4	1.03	29,992	338.5	200,000	18.57	18,590
Case-study #2	27.7	0.88	24,754	472.0	182,000	1.90	1,900

Table 5. Main data referred to the frame's members

	Columns				**Beam**				
	Cross section		**Reinforcement**		**Cross section**		**Reinforcement**		
	b_c	h_c	*As*	*Stirrups*	b_b	h_b	A_{top}	A_{bottom}	*Stirrups*
	mm	**mm**	**No, diam.**	**Diam./ spacing**	**mm**	**mm**	**No, diam.**	**No, diam**	**diam./ spacing**
Case-study #1	127	203	4ϕ10	ϕ5/152	127	197	3ϕ10	2ϕ10	ϕ5/76
Case-study #2	350	350	8ϕ16	ϕ8/100 (150)	350	400	2ϕ16	2ϕ16	ϕ8/100 (150)

mechanical information concerning the infilled systems are listed, while Table 5 shows the data referred to columns and beams.

Furthermore, the stiffness and the shear capacity of the infilled frames have been checked, to relate the "intrinsic" mechanical properties of the assumed strut models, compared to the bare frame ones, to the corresponding properties of the original system. As regards the frame, the stiffness (K_{fr}) has been quantified through a simplified expression, as the sum of the shear-type columns stiffness:

$$K_{fr} = 2\left(12\,E_c I_c/h^3\right) \tag{8}$$

whilst the shear capacity of the frames, V_{fr}, has been found as the product of the columns sections and the shear stress (τ_c), assumes according to ACI 318-02 (American Concrete Institute, 2002) ($\tau_c = \sqrt{f_c}/6$):

$$V_{fr} = 2\,b_c h_c \tau_c \tag{9}$$

The stiffness of the infill panels (K_{inf}), in turn, has been found after the following expression:

$$K_{inf} = \frac{G_m A_{inf} E_m L_{inf}^2}{h_{inf}^3\,G_m + 1.2\,h_{inf} E_m L_{inf}^2} \tag{10}$$

and its shear capacity (V_{inf}) has been roughly determined as the product of the panel horizontal section and a stress equal to f_m /10.

Figure 5. Assumed stress in the strut-models, f_{str}.

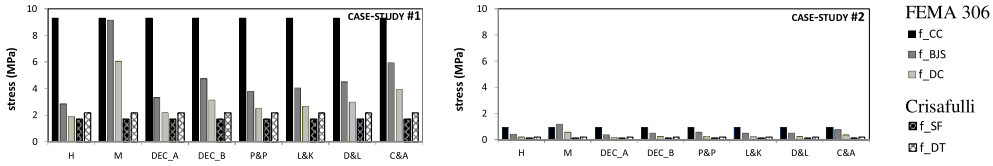

3.2. Data referred to the strut-models adopted for analysis

In Table 6 the width (w) found according to the considered strut-models, presented in § 2.1, have been listed for the two case-studies. Figure 5 shows the stress (f_{str}) values assumed for the strut. It should be noted that some of the considered stress values (provided by FEMA 306 for the diagonal cracking and the bed joint sliding collapse mechanisms) are not defined after the strut model, concerning instead the infill cross section ($A_{inf} = t_{inf}.l_{inf}$); in these cases, therefore, f_{str} is defined as the ratio between the compressive strength of the strut (D_{BJS}, D_{DC}) and the strut cross section, resulting different for each strut-model. The other stress values, instead (provided by FEMA for the *CC* and by Crisafulli for the *BJS* and *DT*), refer directly to the stress to give to the strut. As a consequence, some values of stress are constant for all the models, whilst some others are different for each considered strut width. As should be noted, the *CC* stress is larger than all the others, despite the *BJS* stress has similar (or even larger, for the case-study #2) values when the strut model proposed by Mainstone is adopted, since it leads to assume a strut with a depth much smaller than the other models.

The considered strut-models have been checked even in terms of stiffness (K_{str}) and shear capacity (V_{str}). K_{str} has been quantified as the horizontal component of the axial stiffness of the struts ($E_{inf} A_{str} / D_{inf}$), whilst V_{str} has been found as the horizontal component of their axial capacity ($A_{str} f_{str}$), depending on the assumed stress for the strut.

In Figures 6 and 7 the ratios between strut and frame stiffness and shear capacity have been shown, respectively. As can be noted in Figure 6, the strut stiffness is sensitive to the assumed strut width, and therefore to the considered strut-models, whilst it is not sensitive to the considered stress values, since the same value of Young modulus has been assumed in all cases. In the same figure, the ratio between the stiffness of infill and frame, as defined in Equations (8) and (10), is even shown. The ratio between the strut and the frame shear capacity, instead, is sensitive both to the struts width and stress, as can be observed in Figure 7.

Table 6. Strut width (w) of the strut models of the case-studies (in mm)

Models	H	M	D&F_UN	D&F_CR	P&P	L&K	D&L	C&A
Case-study #1	753	234	645	451	565	528	337	360
Case-study #2	1,274	457	1,427	1,080	955	1,124	650	705

Figure 6. Ratio between the strut and the frame stiffness.

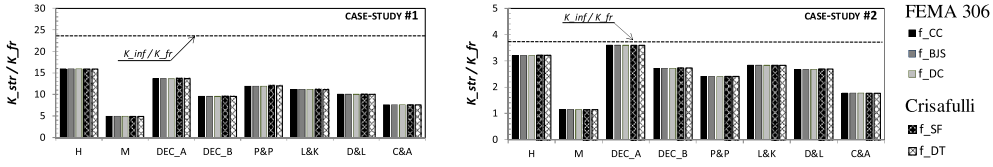

Figure 7. Ratio between the strut and the frame shear capacity.

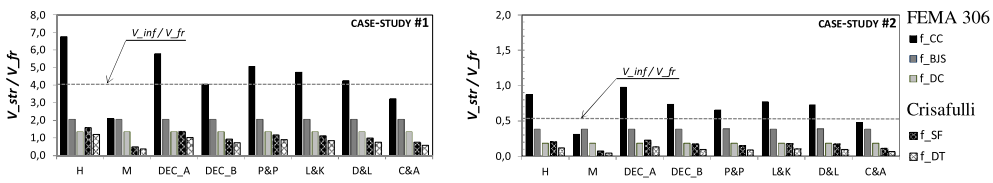

4. The seismic capacity of the case-studies

4.1. The numerical analysis

The Seismostruct platform (Seismosoft, 2006) has been adopted for the analysis. Each frame member has been divided in 4 branches. A fiber model has been assumed for representing the cross sections, where the concrete has been described through the Mander, Priestley, and Park (1988) relationship and the reinforcement has been represented by a bilinear model with a hardening ratio equal to 1%. The diagonal strut behavior has been represented by no-traction links introduced at its ends, described through asymmetric Takeda model. The pushover analysis has been performed by combined force and displacement control.

4.2. Experimental and numerical capacity curves

The capacity curves obtained by performing the numerical analysis have been compared to the experimental ones. Figures 8 and 9 show the obtained capacity curves for the two case-studies,

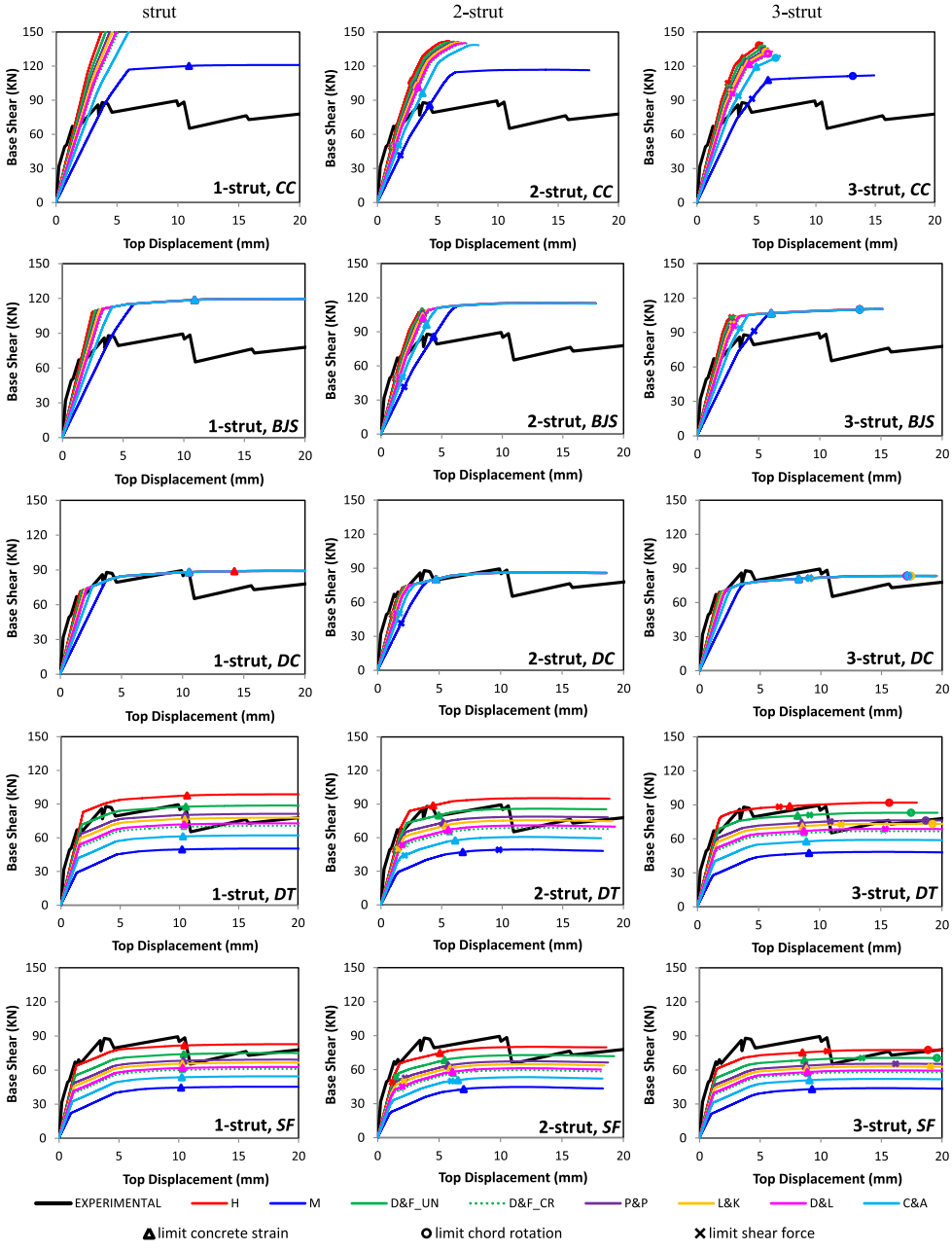

Figure 8. Capacity curves found for the case-study #1.

Figure 9. Capacity curves found for the case-study #2.

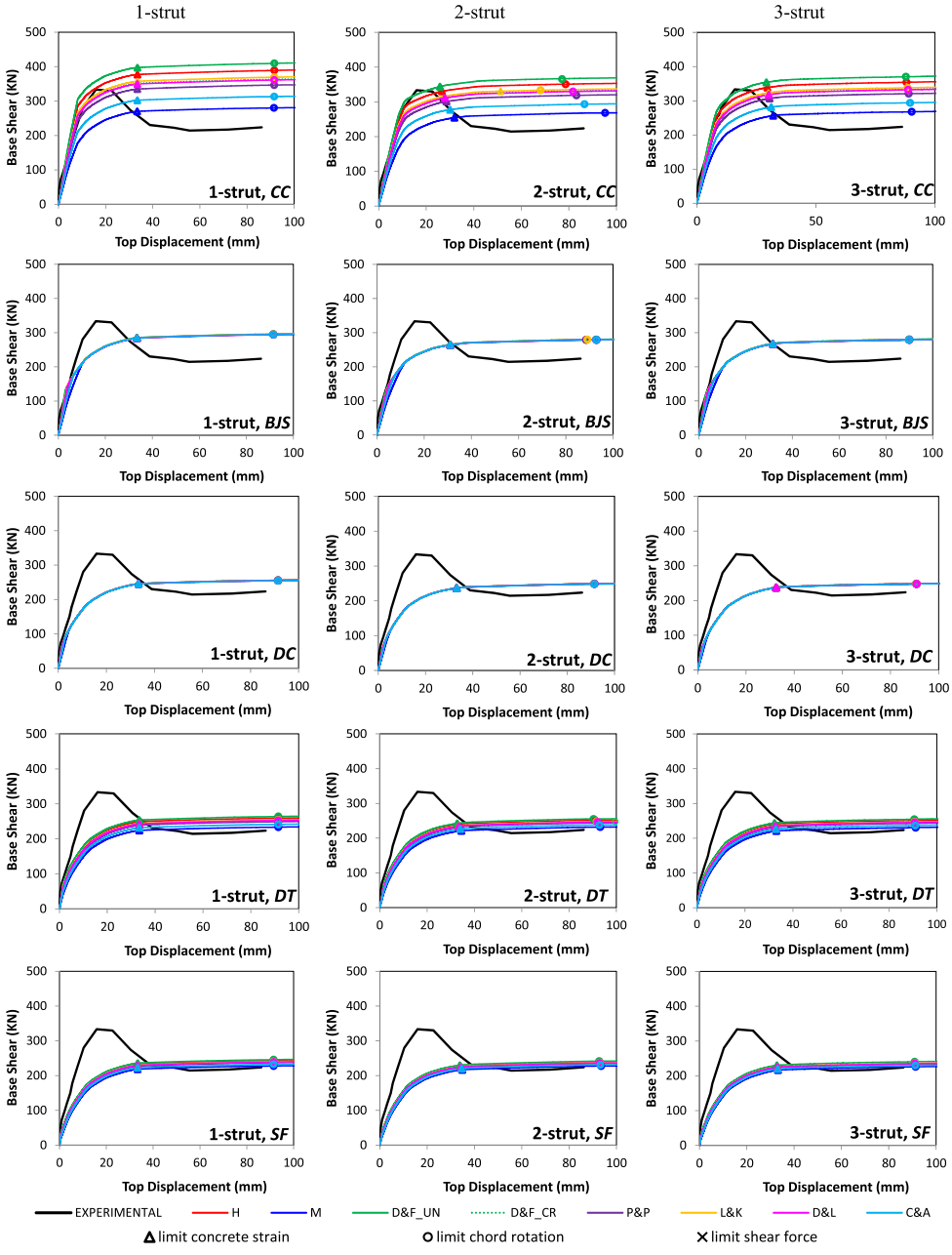

respectively. In each Figure the capacity curves, obtained by adopting the considered models and stress values, have been shown for the models with 1, 2 and 3 struts, respectively. In the same Figures the limit conditions assumed in the analysis, i.e. the achievement of the limit values for the concrete strain, chord rotation and shear force, are shown. All the limit conditions have been taken after the EC8 provisions: the ultimate concrete strain has been assumed equal to 0.0035, the limit chord rotation has been taken as ¾ of the ultimate rotation, defined according to Annex A of EC8 (Equation A1)(EC 8-3, 2005), as well as the limit shear (EC8, Equation A12) (EC 8-3, 2005).

As regards the case-study #1, the strut stress which better represents the experimental results is f_{BJS}, provided by FEMA 306. Since f_{BJS}, as f_{DC}, has been derived for each strut model by the same horizontal force, all models provide the same results in terms of maximum base shear, whilst—as expectable—they differ to each other as regards the elastic stiffness. Even the strut stress values

proposed by Crisafulli (f_{DT}, f_{SF}), which vary very much depending on the considered strut-model, provide an acceptable approximation of the experimental results. The number of struts does not affect very much of the obtained capacity curves, in terms of maximum base shear or top displacement. When the 2-strut model is adopted, however, the collapse mechanism of the system changes, and the limit shear force is achieved in the columns for lower loads than in the other cases.

The case-study #2 differs very much from the #1, as regards the comparison between experimental and numerical results. First of all the stress value more adequate to describe the real behavior of the system is the larger one (f_{CC}), representing the corner crushing of the compressive strut. All the other stress values provide results well below the base shear found experimentally. Furthermore, except for f_{CC}, the system is not sensitive to the strut width, since all the pushover curves are very close each other for all the considered strut-models.

To better compare the numerical results to the experimental one, the elastic stiffness and the maximum base shear provided by the numerical analysis have been checked. Figure 10 shows the comparison in terms of elastic stiffness. Since the stiffness has a degrading trend at the increasing of the system strain even in the first steps of the analysis; the $K_{60,inf}$ values refer to the stiffness corresponding to a base shear equal to 60% of the maximum one, i.e. the stiffness of the equivalent bilinear curves.

As can be noted, all the adopted models underestimate the stiffness of the case-study #1, whilst the stiffness of the case-study #2 is approached, especially when f_{CC} and f_{BJS} are assumed. These results are not surprising, since they are compatible to the comparison made between K_{str} and K_{fr}, shown in Figure 6.

In Figure 11 the maximum base shear provided by the adopted models for the two case-studies has been shown, together with the experimental values. In the Figure, as well as in the following sections, two different values of the base shear are shown, referring, respectively, the maximum values provided by the analysis (V_{max_inf}) and to ones at the achievement of the limit conditions (V_{lim_inf}). In some cases (case-study #1, 2-strut), indeed, the limit conditions imposed to the system are achieved much before the complete development of the inelastic sourced of the frame.

Figure 10. Elastic stiffness of the case-studies.

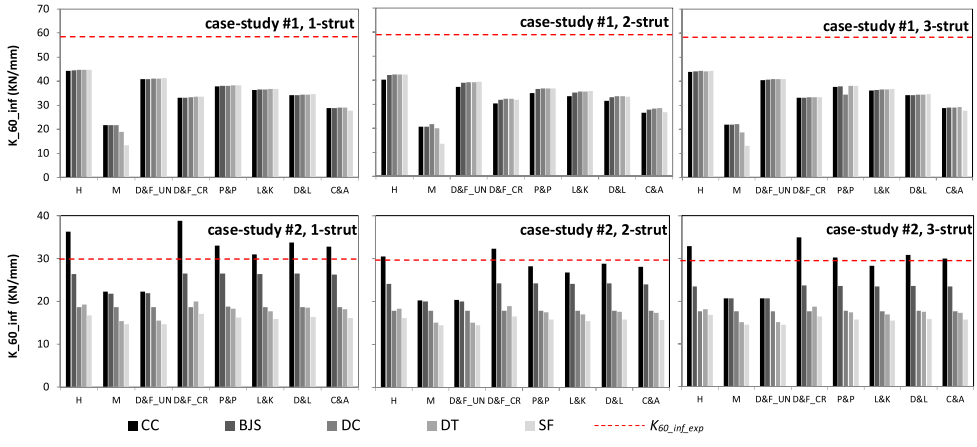

Figure 11. Base shear of the case-studies.

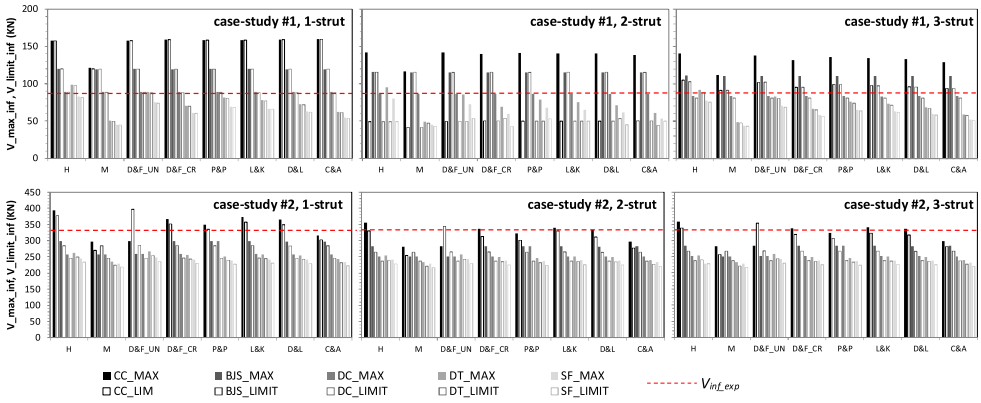

5. Discussion of the obtained results

The results obtained in this work underline the uncertainties in choosing a proper strut model to represent the behavior of infilled frames. The considered case-studies, in fact, evidence many differences in the comparison with the experimental results. As regards the choice of the model, the ones which provide higher width for the strut (H, D&F_UN) seem to better catch the initial stiffness of the frames. As regards the choice of the stress to assume for the strut, the case-study #1 is better represented by the lowest values (f_{DC}, f_{DT}, f_{SF}), whilst the case-study #2 is better simulated by assuming the higher strut stress f_{CC}. Finally, the number of struts to represent the panel does not significantly affect the capacity curves, resulting however to be important for the evaluation of the collapse mechanisms of the systems. In this section the role of the main choices related to the strut model have been discussed, and a joint lecture is proposed for the two frames.

5.1. Effects of the model assumptions on the response quantities

The effects of each of the considered assumption has been measured in terms of scatter in the response quantities, i.e. the elastic stiffness, $K_{60,inf}$, and the maximum base-shear, $V_{max,inf}$, for the two case-studies. The scatter has been measured through the percentage difference (% DIFF), defined, for each quantity, according to the following expression:

$$\%\ \text{Diff} = \frac{\text{Max value} - \text{Min value}}{\text{Experimental value}} \tag{11}$$

Figure 12 shows the scatter found for the two case-studies as a function of the strut width, quantified by considering, for each stress value and number of struts, the maximum and the minimum values provided by the considered strut-models. As can be noted, the stiffness of the case-study #2 is sensitive to the strut width only when the *CC* stress is adopted, evidencing a scatter below 10% in all the other cases. The stiffness of the case-study #1, instead, is sensitive to the strut width in all cases (scatter between 30% and 55%). As regards the limit base-shear, it should be reminded that the *BJS* and *DC* stress values have been defined in order to have the same strut strength in all models; consequently all the capacity curves achieve the same amount of base shear, unless achievement of limit conditions.

Figure 13 shows the scatter in the response quantities related to the strength value assumed for the strut. In this case the maximum and minimum values considered to find the scatter refer, for

Figure 12. Effect of the strut width.

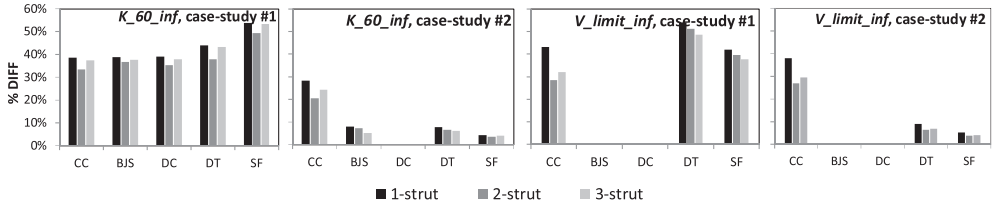

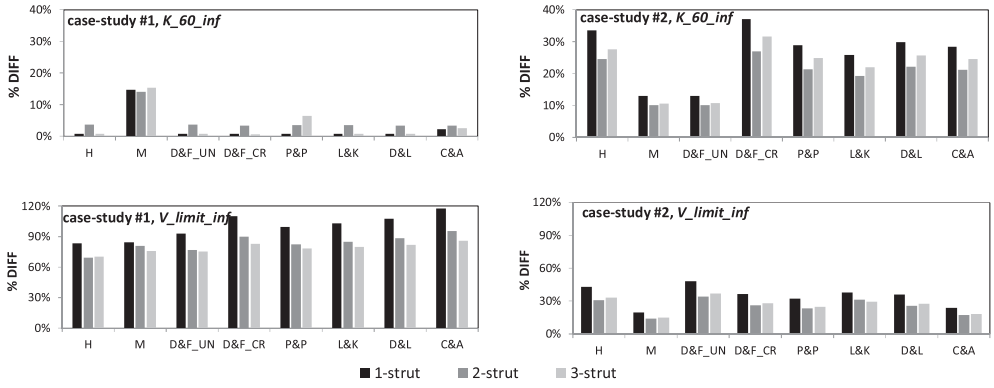

Figure 13. Effect of the strut stress.

each strut model and number, to the results provided by the considered stress values. The case-study #1 evidences a difference sensitivity to the assumed stress in the two response quantities. In fact, the stiffness $K_{60,inf}$ has a negligible sensitivity, except for the M model, which achieves the post-elastic range before 60% of the maximum base shear, where the stiffness is measured. The case-study #2, instead, evidences the same sensitivity to the stiffness and the base shear, with a scatter ranging between 10% and 40% depending on the assumed model.

Finally, the effects related to the number of struts assumed in the model have been checked, and shown in Figure 14. In this case the maximum and minimum values have been found, for each strut model and stress, by considering the three values related to the considered strut number. As can be noted in Figure 14, this assumption is almost negligible for the stiffness, with values of *% DIFF* below 5% (except for the case-study #2, when the *CC* stress is adopted). The number of struts, instead, plays a crucial role in the evaluation of the maximum shear force in the case-study #1. As it was already highlighted, indeed, the number of struts affects the attainment of the limit conditions imposed to the systems; namely, in the case-study #1 the 2-strut model provides a premature failure of the system, comparing to the other models.

5.2. Comparison between the results found for the two case-studies

In order to better understand, and to compare, the results provided by the analysis for the two case-studies, they have been expressed in terms of non-dimensional quantities. Namely, the increase in elastic stiffness (i_K) and in base-shear (i_V) provided by the diagonal strut has been introduced to measure the effect of the infill panel in the considered models. Such increase has been normalized through the maximum quantities of the corresponding experimental test, according to the following relationships:

$$i_K = \frac{K_{\_60\_inf} - K_{\_60\_bare}}{K_{60\_bare\_exp}} \tag{12}$$

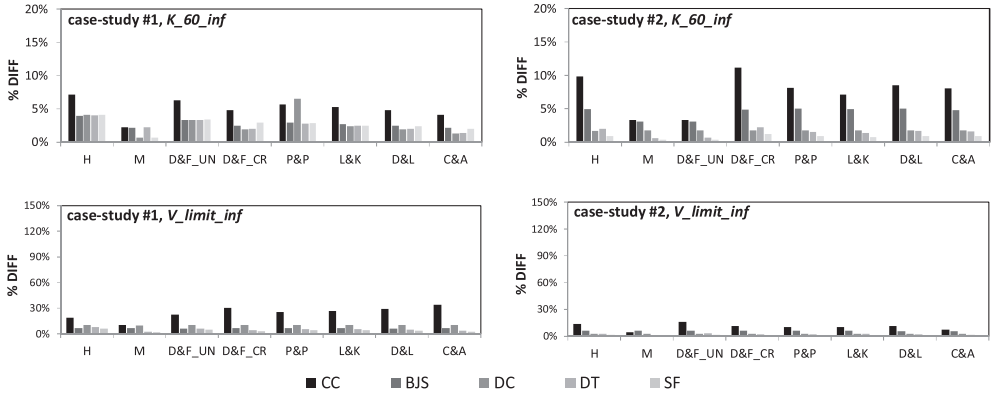

Figure 14. Effect of the strut number.

$$i_{V\_max} = \frac{V_{max\_inf} - V_{bare}}{V_{bare\_exp}} \tag{13a}$$

$$i_{V\_limit} = \frac{V_{limit\_inf} - V_{bare}}{V_{bare\_exp}} \tag{13b}$$

The increase in the response quantities have been related to the amount of stiffness and shear, which have been expressed as the ratio between the strut and the frame quantities (K_{str}/K_{fr}, V_{str}/V_{fr}), as defined in § 3.2 and shown in Figures 6 and 7. The i_K and i_V values obtained through the analysis for the two case-studies are shown in Figures 15–17, together with the "error" of the numerical models. The "error" has been defined in non-dimensional terms, as:

$$\text{Error} = \frac{\text{Response quantity}(\text{numerical}) - \text{Response quantity (experimental)}}{\text{Response quantity (experimental)}} \tag{14}$$

In Figure 15 the increase in stiffness has been shown as a function of the ratio between the strut and the frame stiffness. As should be noted, both case-studies evidence an increase in stiffness at the increasing of K_{st}/K_{fr} ratio, even if the case-study #1 presents an i_K amount much larger than the case-study #2. In the same figure the error trend is shown. As regards the case-study #1, all the strut models provide a stiffness increase well below the experimental value, and the error is over 20% in all cases. In the same diagram the ratio between the infill and the frame stiffness—as listed in Figure 4—is shown. All the strut models have a stiffness much smaller than the infilled one. The Holmes model, which has the higher stiffness, provides the best approximation of the experimental result. As regards the case-study #2, the strut models provide a similar stiffness to the infill panel, and several strut-models approach the experimental result with a satisfactory approximation, when the FEMA strut stress values (f_{CC}, f_{BJS}, f_{DC}) are applied. The quality of the results can be evaluated even by checking the ratio between the infill and the frame stiffness, evidenced in the graphs. In both cases the K_{inf}/K_{fr} quantity corresponds to good results comparing to experimental ones.

Figures 16 shows the increase in base shear provided by the considered strut models. Both the maximum shear attained by the whole capacity curves (max shear) and the value at the achievement of limit conditions (limit shear) are represented. The maximum shear, indeed, is more suitable to express the effects of the width and stress assumptions made for the struts, whilst the limit shear provides important information about the role plaid by the strut number. As regards the case-study #1, there is a good proportionality between i_V and V_{str}/V_{fr} for V_{str}/V_{fr} below 3.0. For larger shear amount,

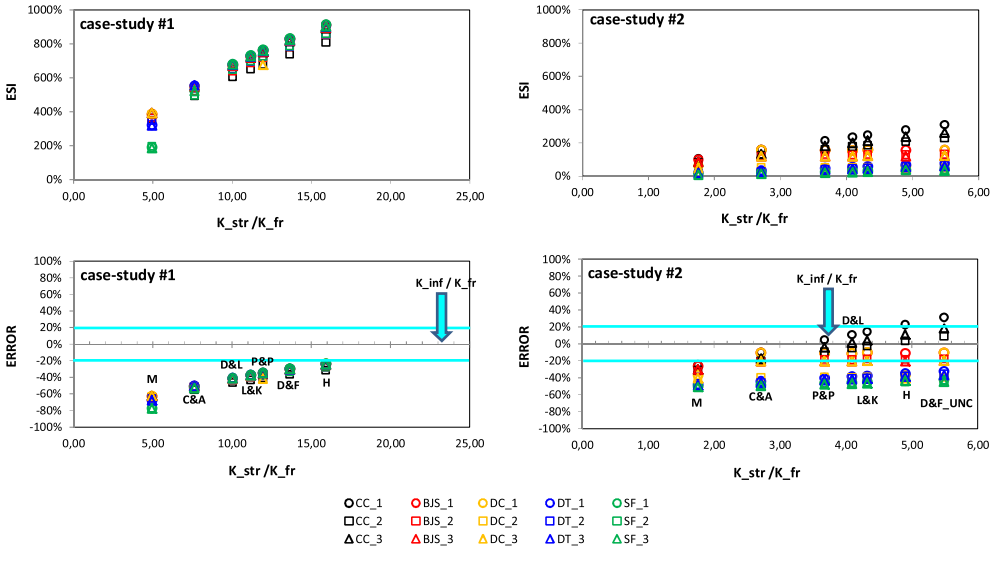

Figure 15. Increase in stiffness of the two case-studies.

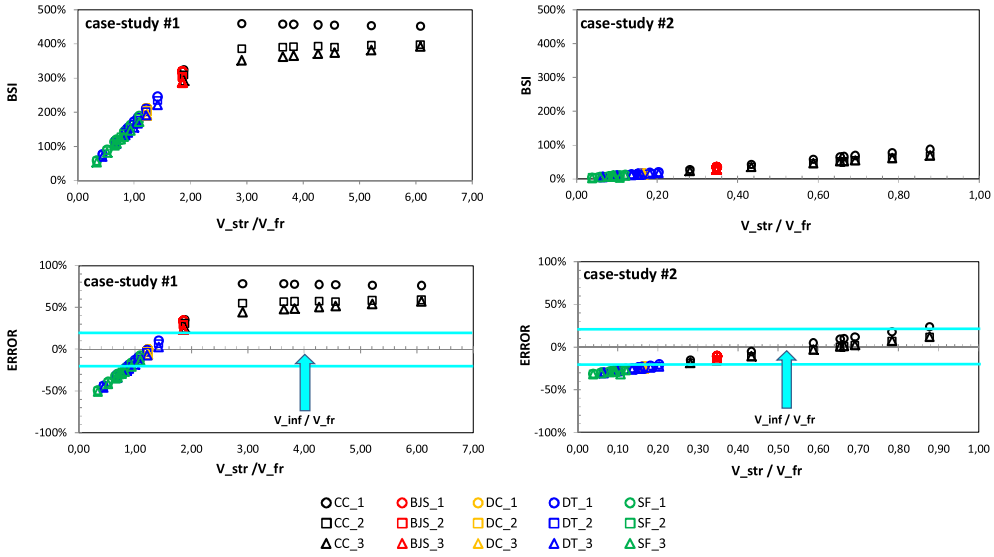

Figure 16. Increase in the base shear of the two case-studies (max shear).

this proportionality vanishes, and the i_V keeps the same value, whichever strut stiffness is considered.

By comparing the diagrams of i_V to the ones expressing the "error", it can be noted that the numerical results which better approach the experimental results have V_{str}/V_{fr} values between 0.8 and 1.5. By comparing the diagrams expressing the error values for "max" and "limit" base shear, shown in Figure 17, it can be noted that the results obtained by the 3-strut models are "better", i.e. closer to the experimental ones. Even when the "stronger" strut mode is adopted (H model combined to f_{CC}) the overestimation of the system capacity is corrected by the achievement of the introduced limit conditions.

In the case-study #2, V_{str}/V_{fr} keeps always below 1, and the proportionality between i_V and V_{str}/V_{fr} works for all the obtained results. Even in this case, the f_{BJS} and the f_{DC} results do not follow strictly such proportionality, since at the varying of the strut width the contribution of the infill remains constant, due to the already mentioned stress quantification. Even for the i_V, the obtained results can be compared to the V_{str}/V_{fr} ratio. In the case-study #1 this quantity corresponds to unacceptable results; this evidence suggests that, whichever the panel capacity can be, the adoption of a strut model requires a strut capacity below the double of the frame capacity. The i_K and the i_V values

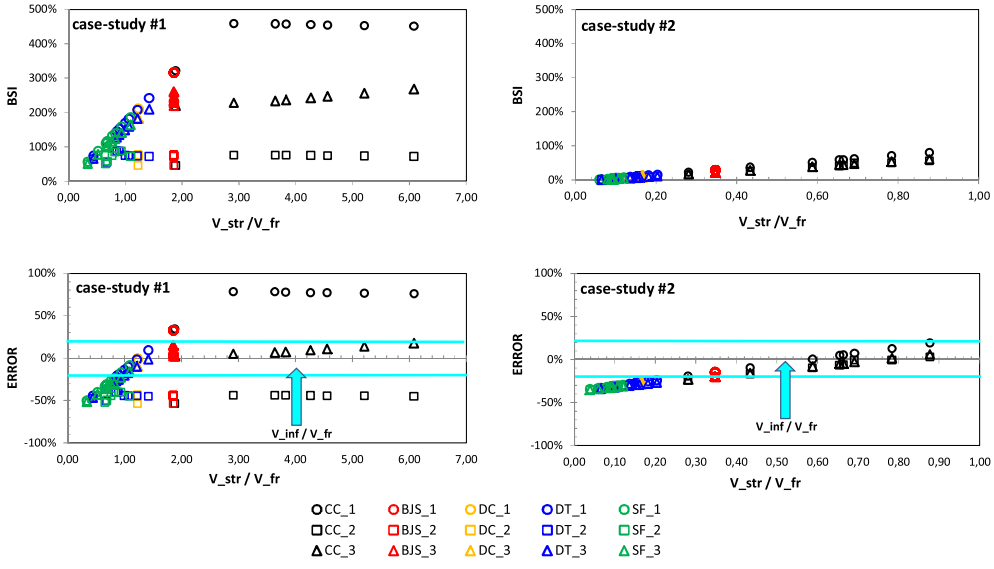

Figure 17. Increase in the base shear of the two case-studies (limit shear).

Figure 18. Comparison between the two case-studies.

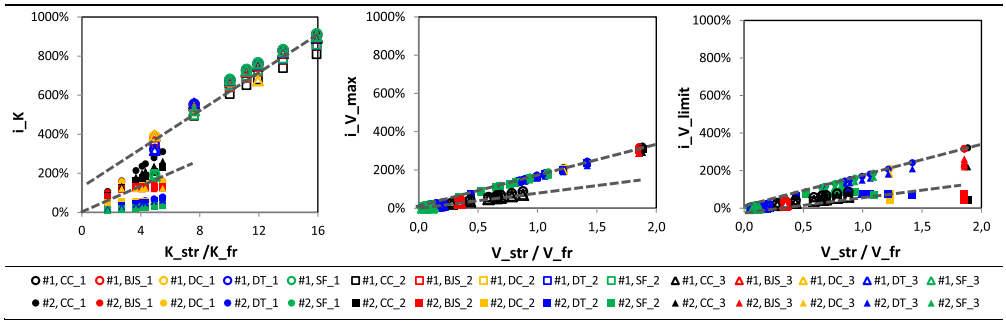

obtained for the two case-studies have been compared in Figure 18. As regards i_V, only V_{str}/V_{fr} values below 2.5 have been considered. As should be noted, both i_K and i_V—when expressed in terms of V_{max}—evidence a strong proportionality to the assumed reference quantities. As can be noted, each case-study presents a different proportionality factor; this difference is not surprising, since they differ very much for the relative contribution of the infill.

6. Conclusive remarks

In this work a numerical analysis has been performed to simulate the seismic response of two different infilled frames, differing for dimensions and mechanical properties and—above all—for the relative stiffness and strength of the infill panel comparing to the frame ones. The effects of the variation in the main properties of the strut model, i.e. the strut width, stress and number, have been checked in terms of elastic stiffness and maximum base-shear of the infilled frames.

According to the obtained results, the following observations can be made:

- all the checked parameters, i.e. strut width, stress and number, affect very much the obtained results;
- the adopted strut-model should fit as much as possible the replaced panel in terms of relative stiffness and shear capacity between panel (strut) and bare frame;
- the shear capacity of the strut cannot exceed a value equal to 2–3 times the one of the bare frame;
- the three-strut models provide a better representation of the panel contribution, reducing eventually the overestimation of its capacity, when a too high stress is assumed for the strut.

In order to achieve more general results, the suggested “input quantities” should be checked on a larger number of samples.

Notes about the article

- Various strut models, differing for width, stress and number have been applied
- Two different case-studies have been assumed for comparison
- Some mechanical parameters expressing the infill contribution have been selected
- The response of each frame has been checked in terms of stiffness and shear
- The suitability of each model has been checked through the selected parameters

Funding
The authors received no direct funding for this research.

Author details
Marco Tanganelli[1]
E-mail: marco.tanganelli@unifi.it
ORCID ID: http://orcid.org/0000-0002-3392-5662
Tommaso Rotunno[1]
E-mail: tommaso.rotunno@unifi.it
ORCID ID: http://orcid.org/0000-0003-4893-9001
Stefania Viti[1]
E-mail: viti@unifi.it
ORCID ID: http://orcid.org/0000-0003-2143-5380
[1] Department of Architecture (DiDA), University of Florence, via della Mattonaia 14, 50121 Firenze, Italy.

Citation information
Cite this article as: On the modelling of infilled RC frames through strut models, Marco Tanganelli, Tommaso Rotunno & Stefania Viti, *Cogent Engineering* (2017), 4: 1371578.

References

Al-Chaar, G., Issa, M., & Sweeney, S. (2002). Behavior of masonry-infilled nonductile reinforced concrete frames. *Journal of Structural Engineering, 128*(8), 1055–1063. doi:10.1061/(ASCE)0733-9445(2002)128:8(1055)

Ali, H. (2009). *Half Scale Three-Storey Infilled RC Building; A Comparison of Experimental and Numerical Models* (Dissertation for the Master Degree in Earthquake Engineering). IUSS, Pavia.

Alva, G. M. S., Kaminski, Jr., J., Mohamad, G., & Silva, L. R. (2015). Serviceability limit state related to excessive lateral deformations to account for infill walls in the structural model. *Revista IBRACON de Estruturas e Materiais, 8*(3), 390–426. doi:10.1590/S1983-41952015000300008

American Concrete Institute. (2002). *ACI building code requirements for reinforced concrete* (ACI 318-02). Farmington Hills: ACI.

Asteris, P. G., Kakaletsis, D. J., Chrysostomou, C. Z., & Smyrou, E. E. (2011). Failure modes of in-filled frames. *Electronic Journal of Structural Engineering, 11*(1), 11–20.

Cavaleri, L., & Di Trapani, F. (2015). Prediction of the additional shear action on frame members due to infills. *Bulletin of Earthquake Engineering, 13*(5), 1425–1454. doi:10.1007/s10518-014-9668-z

Chrysostomou, C. Z., & Asteris, P. G. (2012). On the in-plane properties and capacities of infilled frames. *Engineering Structures, 41*, 385–402. doi:10.1016/j.engstruct.2012.03.057

Crisafulli, F. (1997). *Seismic behaviour of reinforced structures with reinforced masonry infills* (Phd Thesis). University of Canterbury, Christchurch.

Crisafulli, F. J., & Carr, A. J. (2007). Proposed macro-model for the analysis of infilled frame structures. *Bulletin of the New Zealand Society for Earthquake Engineering, 40*(2), 69–77.

Decanini, L. D., & Fantin, G. E. (1986). Modelos simplificados de la mamposteria incluida en porticos. Caracteristicas de rigidezy resistencia lateral en estado limite. *Jornadas Argentinas de Ingenieria Estructural, 2*, 817–836.

Durrani, A. J., & Luo, Y. H. (1994). Seismic retrofit of flat-slab buildings with masonry infills. In *Proceedings of the NCEER Workshop on Seismic Response in Masonry Infills* (Technical Report NCEER 94-004, 3–8). Buffalo, NY: National Center of Earthquake Engineering Research.

EC 8-3. (2005). *Design of structures for earthquake resistance, part 3: Strengthening and repair of buildings, European standard EN 1998-3*. Brussels: European Committee for Standardization (CEN).

El-Dakhakhni, W. W., Elgaaly, M., & Hamid, A. A. (2003). Three-strut model for concrete masonry-infilled steel frames. *Journal of Structural Engineering, 129*(2), 177–185. doi:10.1061/(ASCE)0733-9445(2003)129:2(177)

Fardis, M. N. (Ed.). (1996). *Experimental and numerical investigations on the seismic response of RC infilled frames and recommendations for code provisions* (ECOEST/PREC 8, Report No. 6). Lisbon: LNEC.

FEMA 306. (1998). *Evaluation of earthquake damaged concrete and masonry wall buildings: Basic procedures manual*. Washington, DC: Federal Emergency Management Agency.

FEMA 356. (2000). *Prestandard and commentary for seismic rehabilitation of buildings*. Washington, DC: Federal Emergency Management Agency.

Flanagan, R. D., & Bennett, R. M. (1999). In-plane behavior of structural clay tile infilled frames. *Journal of Structural Engineering, 125*(6), 590–599. doi:10.1061/(ASCE)0733-9445(1999)125:6(590)

Hendry, A. W. (1990). *Structural masonry*. London: MacMillan Education Ltd.

Holmes, M. (1961). Steel frames with brickwork and concrete infilling. *Proceedings of the Institution of Civil Engineers, 19*, 473–478. doi:10.1680/iicep.1961.11305

Liauw, T. C., & Kwan, K. H. (1983a). Plastic theory of infilled frames with finite interface shear strength. *Proceedings of the Institution of Civil Engineers (London), Part 2, 75*(December), 707–723.

Liauw, T. C., & Kwan, K. H. (1983b). Plastic theory of non-integral infilled frames. *Proceedings of the Institution of Civil Engineers (London), Part 2, 75*(September), 379–396.

Liaw, T. C., & Kwan, K. H. (1984). Nonlinear behavior of non-integral infilled frames. *Computer Structure, 18*, 551–560.

Mainstone, R. J. (1971). On the stiffness and strength of infilled frames. *Proceedings of Institution of Civil Engineering,* Supplement (IV), 57–90.

Mainstone, R. J. (1974). *Supplementary notes on the stiffness and strength of infilled frames* (Current Paper CP 13/74). Garston: Building Research Station.

Mander, J. B., Priestley, M. J. N., & Park, R. (1988). Theoretical stress-strain model for confined concrete. *Journal of Structural Engineering, 114*, 1804–1826. https://doi.org/10.1061/(ASCE)0733-9445(1988)114:8(1804)

Mann, W., & Muller, H. (1982). Failure of shear-stressed masonry—An enlarged theory, tests and application to shear walls. *Proceedings of the British Ceramic Society, 30*, 223–235.

Mosalam, K. M., & Ayala, A. (1996). Effect of geometrical configuration on the seismic response of infilled frame. In *11thWorld Conference on Earthquake Engineering* (Number 1675). Mexico: Elsevier.

Paulay, T., & Priestly, M. J. N. (1992). *Seismic design of reinforced concrete and masonry buildings* (p. 744). New York, NY: Wiley. https://doi.org/10.1002/9780470172841

Reinhorn, A. M., Madan, A., Valles, R. E., Reichman, Y., & Mander, J. B. (1995). *Modeling of masonry infill panels for structural analysis* (Technical Report NCEER-95-0018). Buffalo, NY: National Center of Earthquake Engineering Research, State University of New York.

Rodrigues, H., Varum, H., & Costa, A. B. (2010). Simplified macro-model for infill masonry panels. *Journal of Earthquake Engineering, 14*(3), 390–416. doi:10.1080/13632460903086044

Seismosoft. (2006). *Seismostruct version 5.2.2—A computer program for static and dynamic nonlinear analysis of framed structures*. Retrieved from www.seismosoft.com

Sinha, B. P., & Pedreschi, R. (1983). Compressive strength and some elastic properties of brickwork. *International Journal of Masonry Construction, 3*(1), 19–27.

Smyrou, E. (2006). Implementation and verification of a masonry panel model for nonlinear dynamic analysis of

infilled RC frames. Dissertation for the MSc in Earthquake Engineering. *European School for Advanced Studies in Reduction of Seismic Risk (ROSE SCHOOL). Università degli Studi di Pavia*.

Stafford Smith, B. (1966). Behavior of square infilled frames. *ASCE, Journal of Structural Division, 92*(ST1), 381–403.

Stafford Smith, B., & Carter, C. (1969). A method of analysis for infilled frames. *Proceedings of the Institution of Civil Engineers (London), 44*(September/December), 31–48.

Uva, G., Raffaele, D., Porco, F., & Fiore, A. (2012). On the role of equivalent strut models in the seismic assessment of infilled RC buildings. *Engineering Structures, 42*, 83–94. doi:10.1016/j.engstruct.2012.04.005

Verderame, G. M., De Luca, F., Ricci, P., & Manfredi, G. (2011). Preliminary analysis of a soft storey mechanism after the 2009 L'Aquila earthquake. *Earthquake Engineering & Structural Dynamics, 40*(8), 925–944. doi:10.1002/eqe.1069

Zhai, C., Kong, J., Wang, X., & Chen, Z. (2016). Experimental and finite element analytical investigation of seismic behavior of full-scale masonry infilled RC frames. *Journal of Earthquake Engineering, 20*(7), 1171–1198. doi:10.1080/1

Cogent Engineering **(ISSN: 2331-1916) is published by Cogent OA, part of Taylor & Francis Group.**